Asian Journal of Chemistry; Vol. 26, No. 14 (2014), 4493-4498

ASIAN JOURNAL OF CHEMISTRY

http://dx.doi.org/10.14233/ajchem.2014.17464

A Novel Nano-Surfactant $NiFe_2O_4$-Chitosan Nanoparticles Composed and Used in Enhanced Oil Recovery

Q. LIAN and X.F. ZHENG*

College of Chemical Engineering, Hebei Normal University of Science and Technology, Qinhuangdao 066600, P.R. China

*Corresponding author: Tel: +86 24 2027029; E-mail: lianqilianqi517@163.com

Received: 25 February 2014; *Accepted*: 25 April 2014; *Published online*: 5 July 2014; AJC-15504

Different from the traditional surfactants, the novel magnetic $NiFe_2O_4$-chitosan nanoparticles has the advantage of excellent biodegradation and a high level of controllability. The $NiFe_2O_4$ -chitosan nanoparticles with core-shell structure was prepared successfully. The images of TEM and the SEM showed that the cubic-shape magnetic $NiFe_2O_4$ particles were encapsulated by the spherical chitosan nanoparticles. The size of the $NiFe_2O_4$ -chitosan nanoparticles were all below 100 nm. The saturated magnetization of the $NiFe_2O_4$ -chitosan nanoparticles could reach 75 emu/g and showed the characteristics of superparamagnetism at the same time. The evaluation on the interfacial properties of the product showed that the interfacial tension between crude oil and water could be reduce to ultra-low values as low as 10^{-3} mN/m when the magnetic $NiFe_2O_4$-chitosan nanoparticle was used in several blocks in Shengli oilfield without other additives. Meanwhile, the magnetic $NiFe_2O_4$-chitosan nanoparticles possessed good salt-resisting capacity.

Keywords: Magnetic nanoparticles, Surfactants, Superparamagnetism, Interfacial tension, Enhanced oil recovery.

INTRODUCTION

With the rapid development of nanotechnology, magnetic nanoparticles are currently widely studied[1]. Superpara-magnetic iron oxide nanoparticles have attracted researchers in various fields such as physics[2], medicine[3], biology[4] and materials science[5] due to their multifunctional properties such as small size, superparamagnetism and low toxicity[6]. However, the nanoparticles tend to aggregate due to strong magnetic dipole-dipole attractions between particles[7]. At the same time, the capacity for anti-acid[8], anti-alkali[9] and anti-salt[10] of magnetic nanoparticles is in the low level. Recently, the combination of organic and inorganic components at nano-sized level has attracted considerable attention because of the potential applications in many field[11].

Surface-active agents or surfactants are an important class of chemical compounds used in different sectors of modern industry, such as food[12], pharmaceutical[13], cosmetics[14] and petroleum industries[15]. These compounds are able to reduce surface and interfacial tensions, as well as to form and stabilize oil in water (o/w) or water in oil (w/o) emulsions especially in adsorption of oil for enhanced oil recovery[16-18]. Currently, the alkyl benzene sulfonate is widely used in enhanced oil recovery which has serious pollution, difficult to recycling and non-directional movement ability[19,20]. Due to environmental issues and artificial surfactant, the demand for biodegradable surfactants and controlling direction of the microemulsion with surfactants is increasing.

Chitosan is the alkaline deacetylated product of chitin which is derived from the exoskeleton of crustaceans. It is hydrophilic, biocompatible, non-toxic, biodegradable[21-23]. Due to the presence of both hydroxyl and amine groups in its structure, chitosan can be chemically modified to be used as novel separation media. So, chitosan and its derivative have been widely used in the field of medicine, pharmacy and biotechnology. Yang-Chuang Chang and co-workers had prepared carboxymethylated magnetic particles by carboxymethylated the chitosan and bound onto Fe_3O_4 nanoparticles *via* carbodiimide activation. The carboxymethylated chitosan-conjugated Fe_3O_4 nanoparticles were shown to be quite efficient as anionic magnetic nano-adsorbent for the removal of acid dyes and heavy metal ions. Here, we use chitosan as an effective stabilized agent for $NiFe_2O_4$ nanoparticles and we test the ability to reduce the oil-water interfacial tension of the magnetic chitosan particles and the superparamagnetism which has the directional movement ability.

In this paper, magnetic $NiFe_2O_4$-chitosan nanoparticles were obtained using $NiFe_2O_4$ as cores and chitosan as a polymeric shell. The size, structure and magnetic properties of the resultant magnetic nanoparticles were characterized by TEM, SEM, XRD and vibrating sample magnetometer. The binding of chitosan to the magnetic nanoparticles was confirmed by

Fourier transform infrared (FT-IR) spectroscopy. The performance of surface-active was measured by TX-500C full-scale automatic dynamic spinning drop interfacial tension instrument.

EXPERIMENTAL

Glutaraldehyde solution (50 %), span-80, liquid paraffin, petroleum ether, ethanol, glacial acetic acid, sodium hydroxide (NaOH), Span-80, $Ni(NO_3)_2{\cdot}6H_2O$, $Fe(NO_3)_3{\cdot}9H_2O$. All the chemicals were of reagent grade and purified before used and purchased from Kemel chemical reagent Co. Ltd. Chitosan ($M_w = 1 \times 105$, deacetylating degree 95.5 %) were purchased from YuHuan Chemical Company, Zhejiang Province, China. Deionized water was re-deionized (electrical resistivity = 18.9 MΩ cm, 25 °C) and deoxygenated by boiling for 1 h before used.

Synthesis of magnetite: $NiFe_2O_4$ was prepared without any additional stabilizer to control coprecipitation approach that could be found elsewhere. In a typical synthesis, an aqueous mixture of $Ni(NO_3)_2$ and $Fe(NO_3)_3$ was placed into the three-necked flask according to the stoichiometric ratio of $NiFe_2O_4$ at temperature of 90 °C under mechanical stirring (500 rpm). An aqueous solution of NaOH (0.1 mol/L) was added to adjust the pH to 11 at reflux for 1 h. When a light black sedimentation appeared, the crystal growth was allowed to proceed for 2 h with constant stirring (200 rpm) to produce a stable, water-based suspension. The expectant products were isolated from the solvent by an external magnetic field followed by redispersed in deionized water and dried in the drying oven at room temperature.

Preparation of magnetic chitosan nanoparticles: According to mass ratio of $NiFe_2O_4$ and chitosan is 1:4, 0.5g $NiFe_2O_4$ magnetic particles was quickly added into the 40 mL acetic acid solution (5 % v/v) which contained 2 g chitosan. The solution was placed in the ultrasonic reactor for 10 min. At the same time, control the frequency of ultrasonic is 22 KHz and the power is 1000 w to dispersed the chitosan and the magnetic particles uniformly. After that, add 40 mL liquid paraffin and 10 drops of Span-80. Then the solution is placed in the ultrasonic reactor for 0.5 h. In this work, the ultrasonic frequency is 22 KHz and the power is 500 w. To active $NiFe_2O_4$ to get better magnetic properties, the reaction systems were kept at 60 °C for 5 h in a water bath. The cross-linked magnetic chitosan nanoparticles were formed by adding 2 mL of glutaraldehyde and by keeping the same condition for 5 h. After reaction, the prepared nanoparticles was precipitated with centrifugation (8000 rpm for 1 h) and rinsed with ethanol and deioned water for four times. Finally, the prepared nanoparticles were freeze dried for 24 h.

Characterizations of magnetic chitosan nanoparticles: X-ray power diffraction (XRD) measurement was performed using a Bruker D8 diffractometer with monochromatized CuK_α radiation (λ = 1.5426 Å), 40 kV, 30 mA. Fourier transform infrared spectroscopy (FTIR, IRPrestige-21, Shimadzu Inc.) was used to conform the structure of the magnetic $NiFe_2O_4$-chitosan nanoparticles. The magnetic chitosan nanoparticles were studied by transmission electron microscope (TEM, H-7650, Hitachi Inc.) to confirm the size and morphology. The sample of $NiFe_2O_4$-chitosan nanoparticles for TEM analysis was obtained by placing a drop of the nanoparticle dispersed ethyl solution onto a copper micro-grid and evaporated in 20 °C. The surface of the magnetic particles is detected by the scanning electron microscope (SEM, Kyky-2800, Kyky technology Co., Ltd). The elemental analysis of the particles was analyzed by elemental analyzer (Vario EL III, Elementar Inc.). Magnetic measurement were done in a vibrating sample magnetometer (VSM, PPMS-9, Quantum Design). The sample power was placed in a Teflon-coated sample holder and the mass was accurately measured.

Determination of surface-active for products: The $NiFe_2O_4$-chitosan nanoparticles were mixed with 100 mL injected water corresponding to the oil block. Put a drop crude oil (about 0.1 mL) into the mixture and determine the oil-water interfacial tension.

The performance of surface-active depends on the activity to oil-water interface of the products. We use TX-500C full-scale automatic dynamic spinning drop interfacial tension instrument to measure the crude oil in GD-3, GD-4, GD-6,GD-7 oil block from Shengli Oilfield in China after dehydrated and degassed. When injected water interfacial tension changed corresponding to time, the products should be able to reduce the oil-water interfacial tension to 10^{-3} mN/m and below without any other additives. Unless otherwise specified, the surface-active and anti-salt performance was tested in GD-3 from Shengli Oilfield in China after dehydrated and degassed corresponding to injected water. Furthermore, the products accounted for 0.4 % of the injected water.

RESULTS AND DISCUSSION

FTIR: The curves a, b and c in Fig. 1 were the infrared spectroscopy of $NiFe_2O_4$-chitosan nanoparticles, chitosan particles and the $NiFe_2O_4$ particles. As can be seen from the curve a, there was a new absorption peak at 1635 cm^{-1} that was peak of Schiff base absorption peak. That indicated that the glutaraldehyde indeed involved in the cross-linking reaction. The band at 528 cm^{-1} was a characteristic absorption peak of the magnetic $NiFe_2O_4$ particles showed that $NiFe_2O_4$ magnetic particles effectively crosslinked chitosan particles.

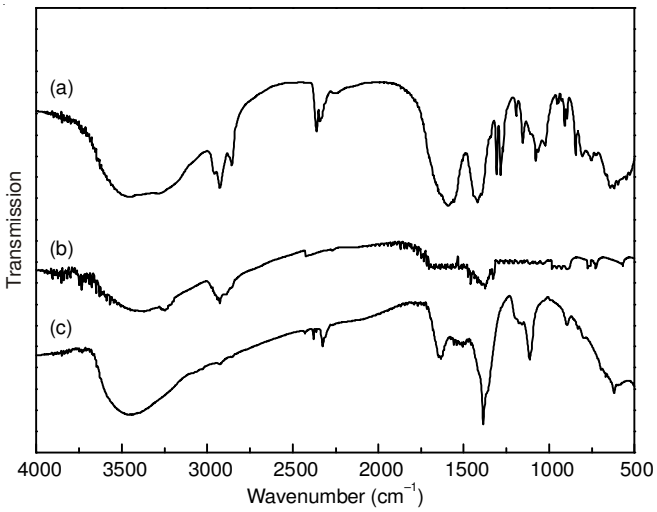

Fig. 1. FTIR spectra of samples: (a) $NiFe_2O_4$-chitosan nanoparticles, (b) chitosan nanoparticles, (c) $NiFe_2O_4$ particles

Contrasting curves a, b and c showed that the curve c contained all the characteristic peaks of the curve a and b, $NiFe_2O_4$ magnetic particles were wrapped by chitosan particles successfully.

XRD: All the diffraction peaks in Fig. 2 confirmed the component of the $NiFe_2O_4$-chitosan nanoparticles. The XRD result of the magnetic chitosan particles and pure $NiFe_2O_4$ particles were mostly coincident. The magnetic chitosan particles were validated as the binding of chitosan and $NiFe_2O_4$.

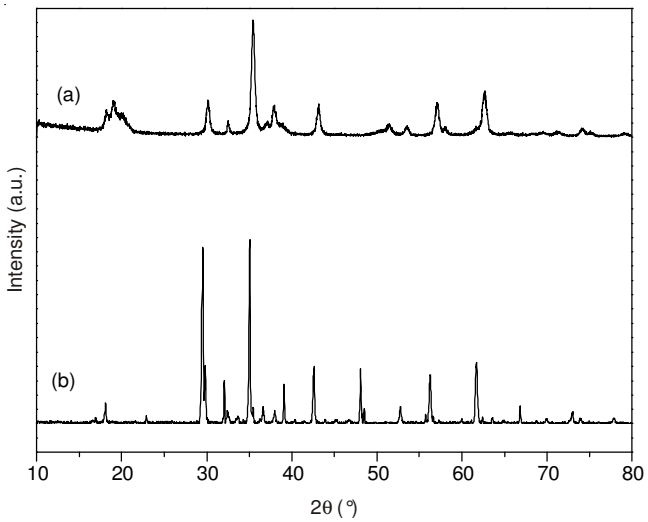

Fig. 2. XRD of cross-link magnetic chitosan nanoparticles: (a) $NiFe_2O_4$-chitosan nanoparticles, (b) $NiFe_2O_4$ particles

TEM: The TEM images of $NiFe_2O_4$ particles (Fig. 3) and $NiFe_2O_4$-chitosan nanoparticles particles (Fig. 4) showed the average diameter of the particles. The size of the $NiFe_2O_4$ particles was varied from 60 to 10 nm. All of the $NiFe_2O_4$ particles were with uniform distribution. In the Fig. 4, we can see that all the magnetic chitosan particles were below 100 nm.

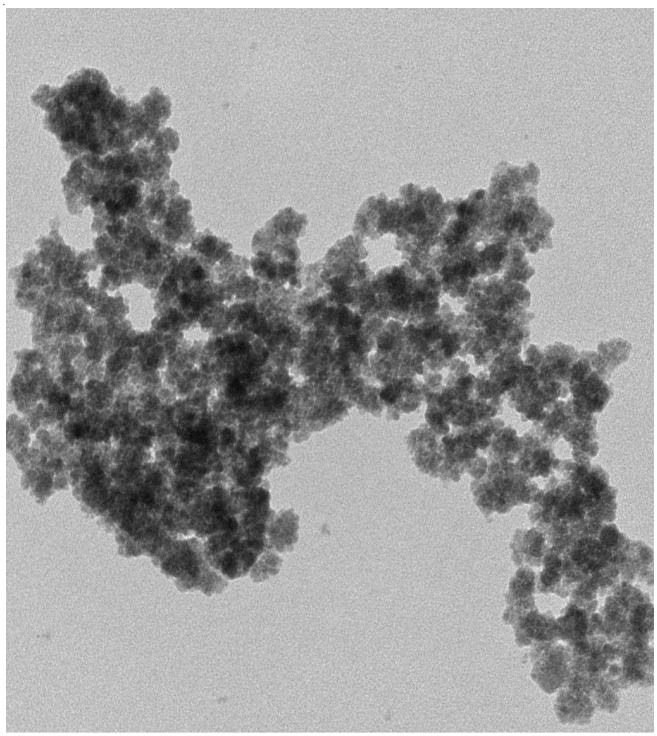

Fig. 3. TEM micrographs for the $NiFe_2O_4$ particles

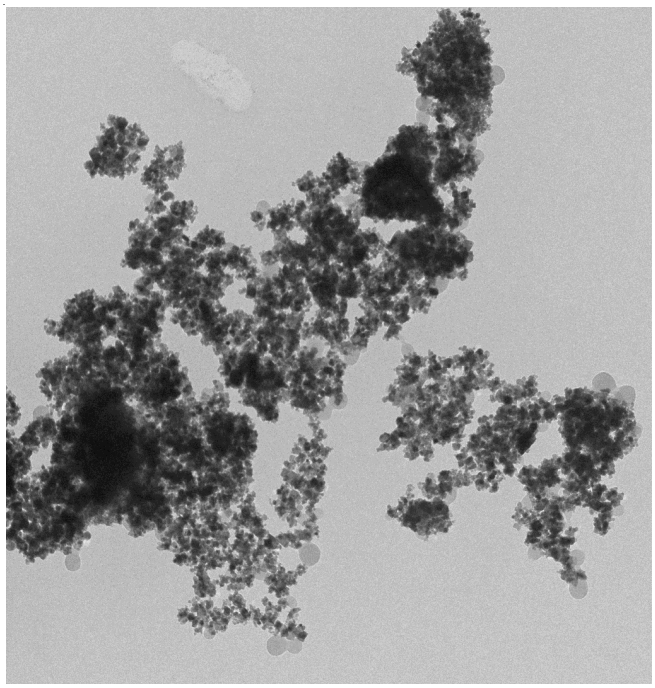

Fig. 4. TEM micrographs for the $NiFe_2O_4$-chitosan nanoparticles

SEM: Figs. 5 and 6 showed the SEM images of the $NiFe_2O_4$ particles and the $NiFe_2O_4$-chitosan nanoparticles. Fig. 5 showed that the $NiFe_2O_4$ particle was under 10 nm and have a spinel crystal structure. Fig. 6 showed the form of the magnetic chitosan nanoparticles. The diameter of the magnetic chitosan particles was about 30 nm and the form varied from the spinel structure of the $NiFe_2O_4$ particle to egg-type shape. From Fig. 6, we can see that the surface of magnetic CS particle was tightly wrapped and didn't have $NiFe_2O_4$ particle. It indicated that the $NiFe_2O_4$ particle was wrapped inside the chitosan successfully.

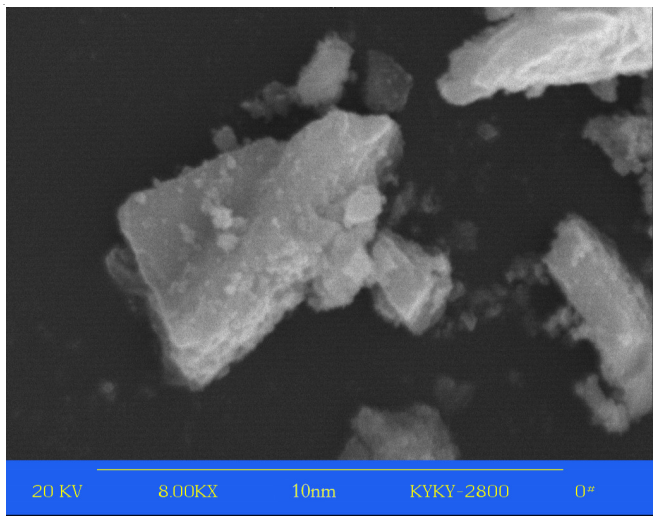

Fig. 5. SEM micrographs for the $NiFe_2O_4$ particles

Elemental analysis result: The data of elemental analysis in the Table-1 show that the Ni, Fe, in the magnetic composite nanoparticles. The atoms ratio of Ni, Fe was about 1: 2 and it indicated that $NiFe_2O_4$ magnetic particles were encapsulated by chitosan particles integrally.

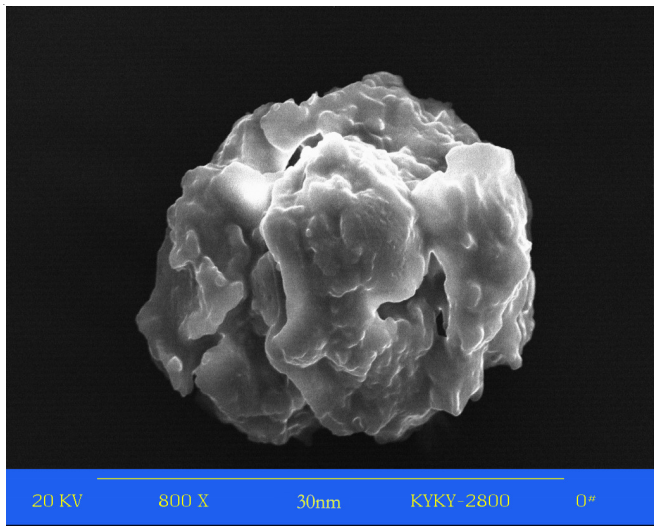

Fig. 6. SEM micrographs for the $NiFe_2O_4$-chitosan nanoparticles

TABLE-1
ELEMENTAL ANALYSIS OF THE
MAGNETIC CHITOSAN PARTICLES

Element	C (%)	O (%)	N (%)	Ni (%)	Fe (%)
Content	48.13	28.56	4.14	6.61	12.56

Magnetization test: For magnetic nanoparticles, one of the distinct behaviors is the occurrence of superparamagnetism which arises from thermal energy overcoming the magnetic anisotropy energy barriers of singledomain particles. The difference between ferromagnetism and superparamagnetism is the particle size. The magnetic moment of the particle change from multi-magnetic domain to mono-magnetic domain and its coercive force enhances with decrease of the scale of particles when the magnetic material is in nano-scale. When the diameter of particles is less than 30 nm, the particles show the character of superparamagnetism[24].

In Fig. 7, the magnetic properties of pure $NiFe_2O_4$ particles and magnetic $NiFe_2O_4$-chitosan nanoparticles were measured. The magnetization of the pure $NiFe_2O_4$ particles was higher than that of the magnetic $NiFe_2O_4$-chitosan nanoparticles. The magnetization of the pure $NiFe_2O_4$ particles was high as 130 emu/g and that of the magnetic $NiFe_2O_4$-chitosan nanoparticles

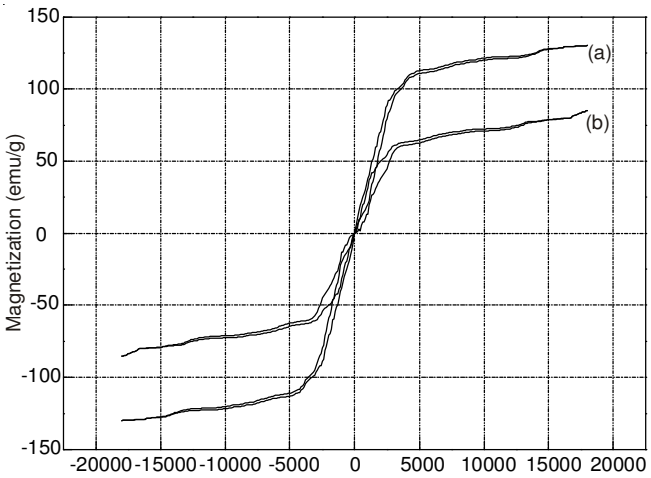

Fig. 7. Field dependence of magnetization for the $NiFe_2O_4$-chitosan nanoparticles (b) and $NiFe_2O_4$ nanoparticles (a)

was 80 emu/g, meanwhile both of the two particles showed the characteristics of superparamagnetism.

The dispersion and magnetic responsive properties of $NiFe_2O_4$-chitosan nanoparticles were vividly given in the Fig. 8. Here, $NiFe_2O_4$-chitosan nanoparticles had a high solubility and dispersibility in water (Fig. 8a) and would not aggregate or precipitate for a least one month. When subjected to a strong magnetic field, the particles could be completely separated from the solution within seconds (Fig. 8b).

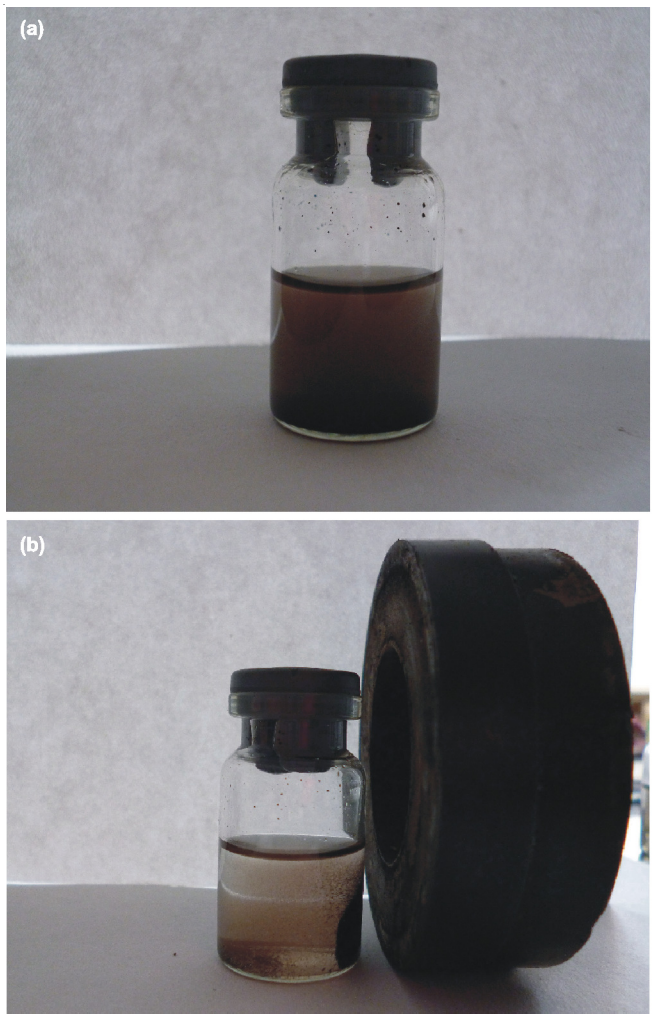

Fig. 8. Optical photograph of the $NiFe_2O_4$-chitosan nanoparticles dispersed in a glass battle: (a) without magnetic field, (b) with magnetic field

Determination of surface-activity

Main properties of injected water: The density of the crude oil in GD-3, GD-4, GD-6,GD-7 oil block from Shengli Oilfield were 0.97, 0.97, 0.89 and 0.91 g/mL. The main properties of the injected water for each block are shown in Table-2.

Determination of surface-activity: We used the TX-500C full-scale automatic dynamic spinning drop interfacial tension instrument to determine the interfacial activity of the products on each oil block. When the measurement time was 1 h, the results were shown in Fig. 9. Apparent from the Fig. 9, the $NiFe_2O_4$-chitosan nanoparticles reduced the oil-water interfacial tension to less than 10^{-3} mN/m in each oil bock without any additives. In particular, the products created minimum oil-water interfacial tension to 5×10^{-4} mN/m in GD-3 and GD-4

TABLE-2
ION CONCENTRATION AND THE TOTAL MINERALIZATION OF THE WATER INTO GD OIL BLOCK

Oil block	Ion concentration (mg/L)					
	Na^+	Ca^{2+}	Mg^{2+}	Cl^-	HCO_3^-	Total mineralization
GD-3	2995.8	207.2	125.9	4831	1437.8	9657.7
GD-4	5164.2	320.8	156.8	10564	480	16685.8
GD-6	9507.2	378.3	210	11186.2	599.1	21980.8
GD-7	7414.1	213.2	268.3	8757.7	819.4	17472.7

with similar nature. The time to reach a stable oil-water interface tension was short and it can reach the ideal interfacial tension value in 5 min generally. Fig. 9 showed that the oil-water interfacial tension were stable. It indicated the products could form a stable flooding system with oil droplets.

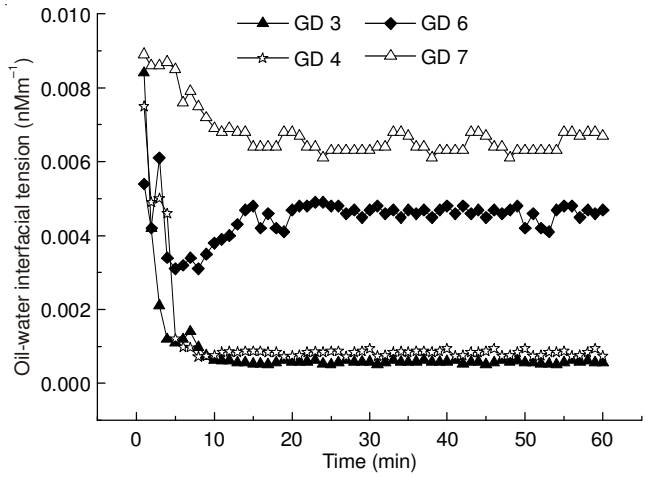

Fig.9. Dynamic interfacial tension of GD oil block

Product concentration influence on oil-water interfacial tension: The impact of the $NiFe_2O_4$-chitosan nanoparticles concentration to oil-water interfacial tension is shown in Fig. 10. When percentage of the products was above 0.3 %, the oil-water interfacial tension can reach 10^{-3} mN/m. But a large number of micelles were formed in the solution when the products mass fraction is higher than 0.4 %. So continued to add products on the basis of the percentage of magnetic chitosan nanoparticles quality had little meaning

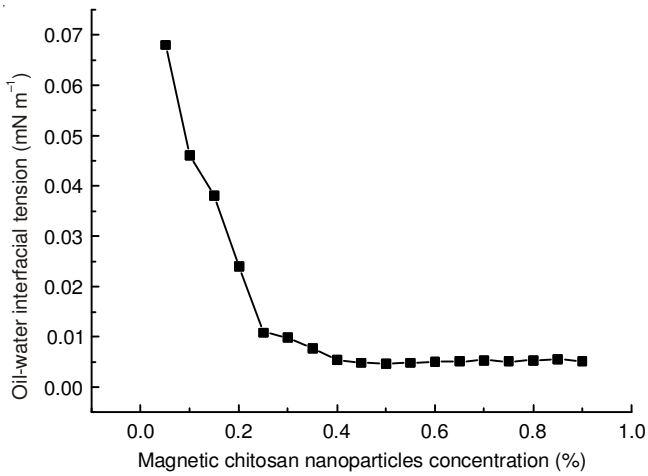

Fig. 10. Effects of $NiFe_2O_4$-chitosan nanoparticles contents on the interfacial tension

Salt-resisting capacity: Because salinity of the injected water from different oil blocks varied widely and it affected the oil-water interfacial tension directly, the $NiFe_2O_4$-chitosan nanoparticles must have good salt-resisting capacity. From the Fig. 11, it is observed that the products could reduce oil-water interfacial tension to 10^{-3} mN/m or less when the NaCl concentration was 2700-16000 mg/L. From that, we know the products had good salt-resisting capacity.

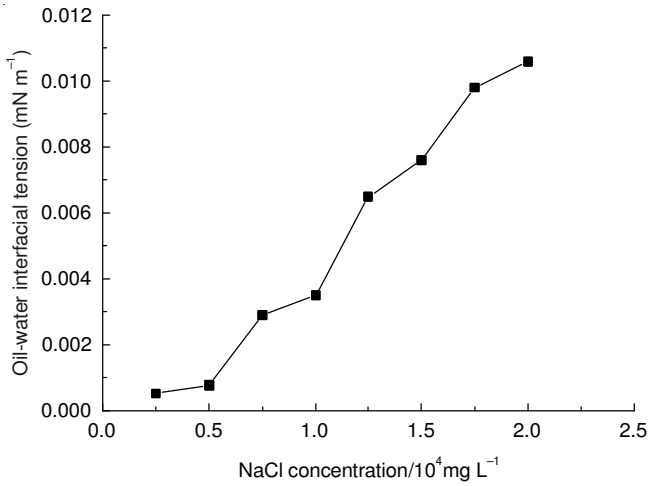

Fig. 11. Effect of sodium ions to interfacial tension

Conclusion

A novel $NiFe_2O_4$-chitosan nanoparticles was composited with excellent core/shell structure and magnetic responsive properties. These superparamagnetic $NiFe_2O_4$-chitosan nanoparticles were able to reduce surface and interfacial tension to 10^{-3} mN/m and below without any other additives. The time to reach a stable oil-water interface tension was short and it can reach the ideal interfacial tension value in 5 min generally. At the same time, the $NiFe_2O_4$-chitosan nanoparticles had good salt-resisting capacity.

ACKNOWLEDGEMENTS

This work was supported by Hebei Education Department Project (Q2012056) and Qinhuangdao Science and Technology Bureau Project (2012021A127).

REFERENCES

1. J.D. Van Hamme, A. Singh and O.P. Ward, *Biotechnol. Adv.*, **24**, 604 (2006).
2. R.S. Makkar, S.S. Cameotra and I.M. Banat, *AMB Express*, **1**, 5 (2011).
3. H.-P. Meyer, *Org. Process Res. Dev.*, **15**, 180 (2011).
4. S.L. Fox and G.A. Bala, *Bioresour. Technol.*, **75**, 235 (2000).
5. L.R. Rodrigues, J.A. Teixeira and R. Oliveira, *Biochem. Eng. J.*, **32**, 135 (2006).
6. J. Roger, J.N. Pons, R. Massart, A. Halbreich and J. Bacri, *Eur. Phys. J. Appl. Phys.*, **5**, 321 (1999).
7. I.M. Banat, R.S. Makkar and S.S. Cameotra, *Appl. Microbiol. Biotechnol.*, **53**, 495 (2000).
8. A. Singh, J.D. Van Hamme and O.P. Ward, *Biotechnol. Adv.*, **25**, 99 (2007).
9. J.D. Desai and I.M. Banat, *Microbiol. Mol. Biol. Rev.*, **61**, 47 (1997).
10. E. Carrero, N.V. Queipo, S. Pintos and L.E. Zerpa, *J. Petrol. Sci. Eng.*, **58**, 30 (2007).
11. M. Nitschke, S.G.V.A.O. Costa and J. Contiero, *Biotechnol. Prog.*, **21**, 1593 (2005).

12. S. Mukherjee, P. Das and R. Sen, *Trends Biotechnol*., **24**, 509 (2006).
13. Y. Wu, J. Guo, W.L. Yang, C.C. Wang and S.K. Fu, *Polymer*, **47**, 5287 (2006).
14. H.W. Gu, K.M. Xu, C.J. Xu and B. Xu, *Chem. Commun.*, 941 (2006).
15. P. Wunderbaldinger, L. Josephson and R. Weissleder, *Bioconjug. Chem*., **13**, 264 (2002).
16. W. Wang, L. Deng, Z.H. Peng and X. Xiao, *Enzyme Microb. Technol*., **40**, 255 (2007).
17. W.S.W. Ngah, S. Ab Ghani and A. Kamari, *Bioresour. Technol*., **96**, 443 (2005).
18. A.J. Varma, S.V. Deshpande and J.F. Kennedy, *Carbohydr. Polym*., **55**, 77 (2004).
19. Y.C. Chang and D.H. Chen, *Colloid Interface Sci*., **283**, 446 (2005).
20. C. Shen, H. Chen, S. Wu, Y. Wen, L. Li, Z. Jiang, M. Li and W. Liu, *J. Hazard. Mater*., **244-245**, 689 (2013).
21. A.C. Zimmermann, A. Mecabo, T. Fagundes and C.A. Rodrigues, *J. Hazard. Mater*., **179**, 192 (2010).
22. R.B. Hernández, A.P. Franco, O.R. Yola, A. López-Delgado, J. Felcman, M.A.L. Recio and A.L.R. Merce, *J. Mol. Struct*., **877**, 89 (2008).
23. G. Zhao, J.J. Xu and H.Y. Chen, *Electrochem. Commun*., **8**, 148 (2006).
24. L. Josephson, Coated with a Polysiloxane and Coupled to a Nucleic Acid, US Patent 4,672,040 (1987).